Stochastic Environmental Research and Risk Assessment 14 (2000) 275–295 © Springer-Verlag 2000

From GCM scales to hydrological scales: rainfall variability in West Africa

T. Lebel, F. Delclaux, L. Le Barbé, J. Polcher

Abstract. The variability of rainfall is a key component determining how the continental surfaces react to the atmospheric forcing. When studying the impact of climatic fluctuations onto the water resources, it is thus of paramount importance to evaluate to which extent the atmospheric models used in this kind of studies are able to reproduce the variability of the rain process, both in space and time. First among these are the general circulation models (GCM) with coarse resolution, which has two consequences: (i) a simplified parametrisation of convection; (ii) a scale of representation of rainfields which is not adequate when it comes to use them as inputs to hydrologic models. Since linking GCM's and regional hydrologic models is the corner stone of impact studies, it is necessary to analyse the consequences of this gap in scales and to find ways of bridging it. As a preliminary step in that direction, a comparative analysis of the observed and of the GCM rainfall variabilities is carried out for a tropical semi-arid zone of West Africa displaying a high sensitivity to climatic fluctuations. Over tropical regions the GCM used here (LMD-6) has a space resolution of 1.6° in latitude and of 3.75° in longitude. The comparative study shows that the errors of the GCM rainfall outputs may be traced down to two fundamental shortcomings: (i) a wrong seasonal cycle, probably linked to problems in representing the large scale circulation; (ii) an unrealistic

T. Lebel (✉), L. Le Barbé
Laboratoire d'Etude des Transfers en Hydrologie et Environnement, BP 53, F38041 Grenoble cedex 9, Paris

F. Delclaux
Hydro Sciences Montpellier, Montpellier, Paris

J. Polcher
Laboratoire de Météorologie Dynamique, Paris

We gratefully acknowledge people in charge of producing the GCM runs at LMD. The surface data used in this study, whether originating from the national raingauge networks or from the EPSAT-Niger experiment, could not have been collected without the constant help and collaboration of Direction de la Météorologie Nationale (DMN) du Niger. Special thanks are owed to Mr A. Also, present director of DMN-Niger, for a long standing and fruitful collaboration extending over more than 10 years. Support from IRD (ex ORSTOM) was also a key component. The study has been partly funded by the French Programme National de Recherche en Hydrologie (PNRH), grant no. 205.

simulation of the mesoscale convective systems that are responsible for 90% of the rainfall over this area. This latter problem is especially damaging from an hydrological point of view, as shown from a detailed analysis of high resolution rainfall observations. Even though it is possible to design rainfall desaggregation models producing realistic small scale rainfields from large scale rainfields, such models are of limited utility as long as atmospheric models are not able to produce a realistic climatology in term of number and magnitude of convective systems.

1 Introduction

Rainfall results from a series of mechanisms spanning a wide range of scales, from synoptic circulations to microphysics. An explicit representation of all these mechanisms in a single model is presently not possible, for both numerical and conceptual reasons. Beside this, hydrologists interested in studying the potential impact of climate variability on water resources face another scale related problem: the gap separating the usual resolution of general circulation models (GCM) and the resolution of hydrologic models. Since GCM's are the only available tool to represent the climatic system and its fluctuations, hydrologists must learn how to make as best a use as possible of their outputs. A first step in that direction is to evaluate how rainfall variability is depicted depending on the scales involved and also depending on whether using observations or model's outputs.

Nowhere more than in West Africa is such an investigation needed. The water resources of this region are especially sensitive to rainfall fluctuations, for there is a permanent imbalance between precipitation and potential evapotranspiration. This was most dramatically illustrated by the recent drought that struck the region for almost 30 years. The available observations (Fig. 1) are not sufficient to diagnose whether this drought is only a low probability event in a globally stable climate or the premise of a long lasting change. Whether atmospheric models can tell us more on that matter is not proven. There are significant differences among GCM's regarding tropical rainfall and hydrologists can only wonder to which extent they should be trusted to help them either in assessing the probability of future droughts, comparable to the recent one, or in simulating credible scenarios that have never occurred in the records.

There are two sources of differences between GCM rainfields and observed rainfields. One is related to the parametrisation of rainfall processes in the GCM's as well as to other simplifications in the representation of atmospheric processes that, in the end, may affect the rain producing conditions. The other source of discrepancy is directly linked to the scale issue, the modes of rainfall variability being heavily dependent on the scale of observation. This paper describes a preliminary investigation to evaluate these two factors.

In Sect. 2, the rainfall variability in West Africa will be analysed in term of fluctuations in the occurrence rate and magnitude of the convective systems. In Sect. 3, the observed rainfall is compared with the GCM outputs for various time scales. In Sect. 4, it is argued that the convective systems are the key link between climatic scales and hydrological scales, while Sect. 5 focuses on the climatology of the convective systems in the GCM. In conclusion we discuss the bearings of the above results in the perspective of climate variability impact studies.

2 The observed climate variability in West Africa

In a study carried out on the Central Sahel, Le Barbé and Lebel (1997) have shown that the drought that started in the end of the sixties was characterised by an overall decrease of the number of rain events. At the same time it appeared that the rain efficiency of the convective systems associated with these events, as measured by the interannual average event rainfall did not vary much. The study was latter extended to a larger area including the continuum of the West African climates from the Guinea Gulf (4°N) to the northern edge of the Sahel (16°N) and from the Guinean forests (10°W) to West Nigeria (4°E).

Based on more than 300 daily reading raingauges covering this 14° × 12° area, the study focused on comparing the rainfall regime of wet and dry years over the region. Indeed the contrast – observed in Fig. 1 for the Sahel – between a 20-year wet period covering the 50's and the 60's, on the one hand, and a 20-year dry period covering the 70's and the 80's seems to apply to the whole region. Comparing the average annual rainfall of the wet period P_1 (1951–1970) to the average annual rainfall of the dry period P_2 (1971–1990) shows an average difference of 180 mm, relatively evenly distributed in space, except for a zone of higher deficit covering the coastal area of Ivory Coast (Fig. 2). Over the Sahel the drought lasted until 1997, with the only exception of 1994. To the south a more complex pattern of interannual variability was recorded. Limiting our study to the years 1951–1990, thus provides us with a period over which there is a clear predominant decadal mode of variability over the whole region (see e.g. Janowiak, 1988; Hastenrath, 1990; Janicot, 1992; Kushnir, 1994; Fontaine and Janicot, 1996; for an analysis of the decadal variability of the rainfall in West Africa and its connection with the variability of the sea surface temperature in the tropical oceans). As shown by Fig. 1 the interannual variability is not negligible either. Consequently, in Sect. 3 below these two modes will be looked at in the LMD-GCM simulations.

Using the model described in Le Barbé and Lebel (1997), the daily rainfall signal R_d is deconvoluted in an event rainfall signal at each station as shown in Fig. 3 for a coastal station (Cotonou) and for a Sahelian station (Niamey). This signal is characterised by two parameters: the average number of events (n) and the average rainfall produced by these events (h). In Fig. 3 the two signals are averaged over 10-day consecutive periods and compared to the 10-day rainfall signal computed by directly accumulating the daily measurements. It clearly appears that most of the decrease in rainfall observed between the wet period and the dry period is related to a decrease in the average number of rain events, especially during the peak of the Sahelian rainy season and during the first rainy season on the coast. The second rainy season shows a similar trend. Its timing is

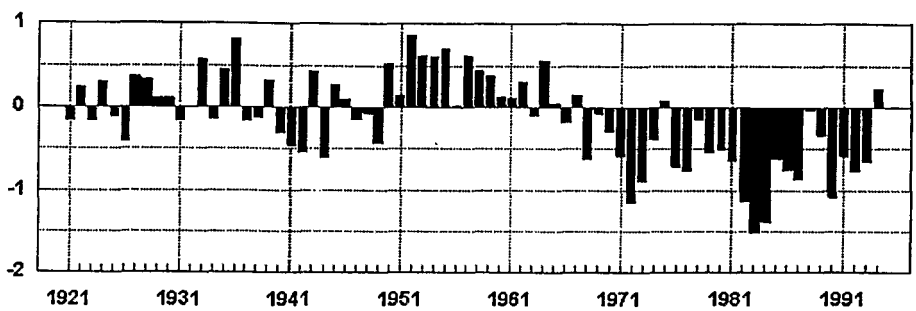

Fig. 1. Evolution of the standardised rainfall index over the Sahel between 1921 and 1994

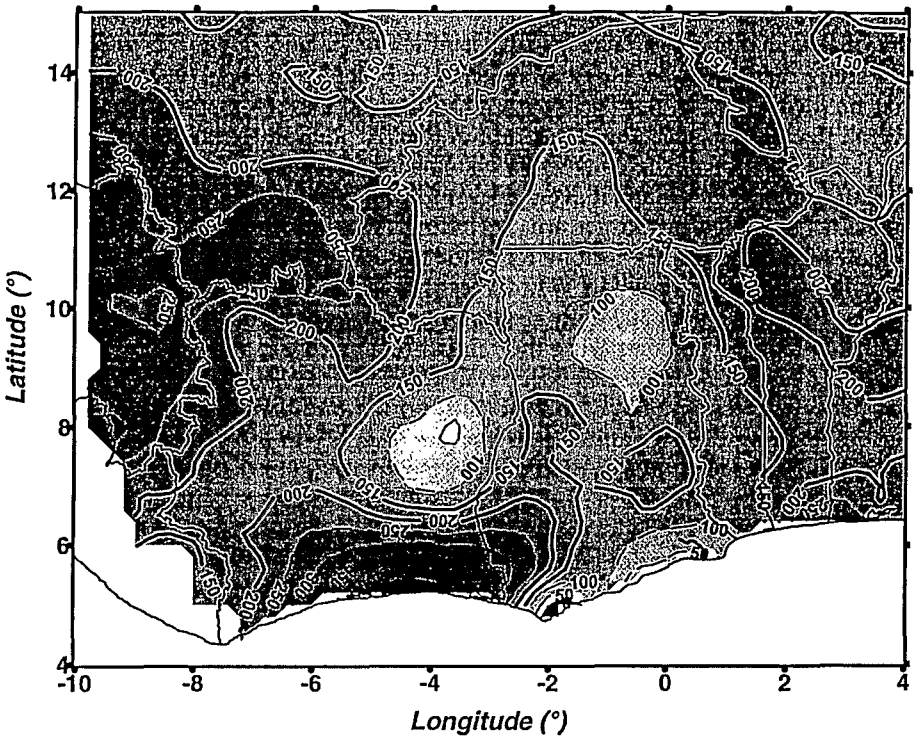

Fig. 2. Map of the decrease (in mm) of the average annual rainfall between the wet period P_1 (1951–1970) and the dry period P_2 (1971–1990)

also affected: it starts earlier and finishes earlier during the dry period than during the wet period. By comparison the average event rainfall displays little significant modifications, except in July and August for Cotonou.

Looking at a broader scale, Fig. 4 illustrates the overall relationship between the decrease of the annual rainfall and that of the average number of events. This figure was obtained by averaging the 3 signals (R_d, n and h) at the yearly scale to obtain the three variables R_Y, n_Y and h_Y and then computing the following index of relative variation:

$$\Delta_X = [X(P_1) - X(P_2)]/X(P_2)$$

where $X(P_i)$ is the average over period P_i of either one of the three variables R_Y, n_Y or h_Y.

Mapping Δ_X, we are able to compare the spatial patterns of fluctuation for the three variables. The spatial view provides a confirmation of the results obtained at the local scale in Fig. 3. Over the Sahelian band (North to 10°N) there is a striking similarity between the map of Δ_R and the map of Δ_n while the map of Δ_h displays low values that are barely significant and non-organised in space. More to the south the situation is that of a gradual change towards the dominant patterns of the coastal climate. Over the Sahel, it may be estimated that between 70% and 80% of the rainfall decrease is associated with the decrease of the number of rain events.

In the following the analysis will focus on the Sahel. The rainfall deficit in this area is larger, relatively to the interannual mean, than elsewhere in West Africa

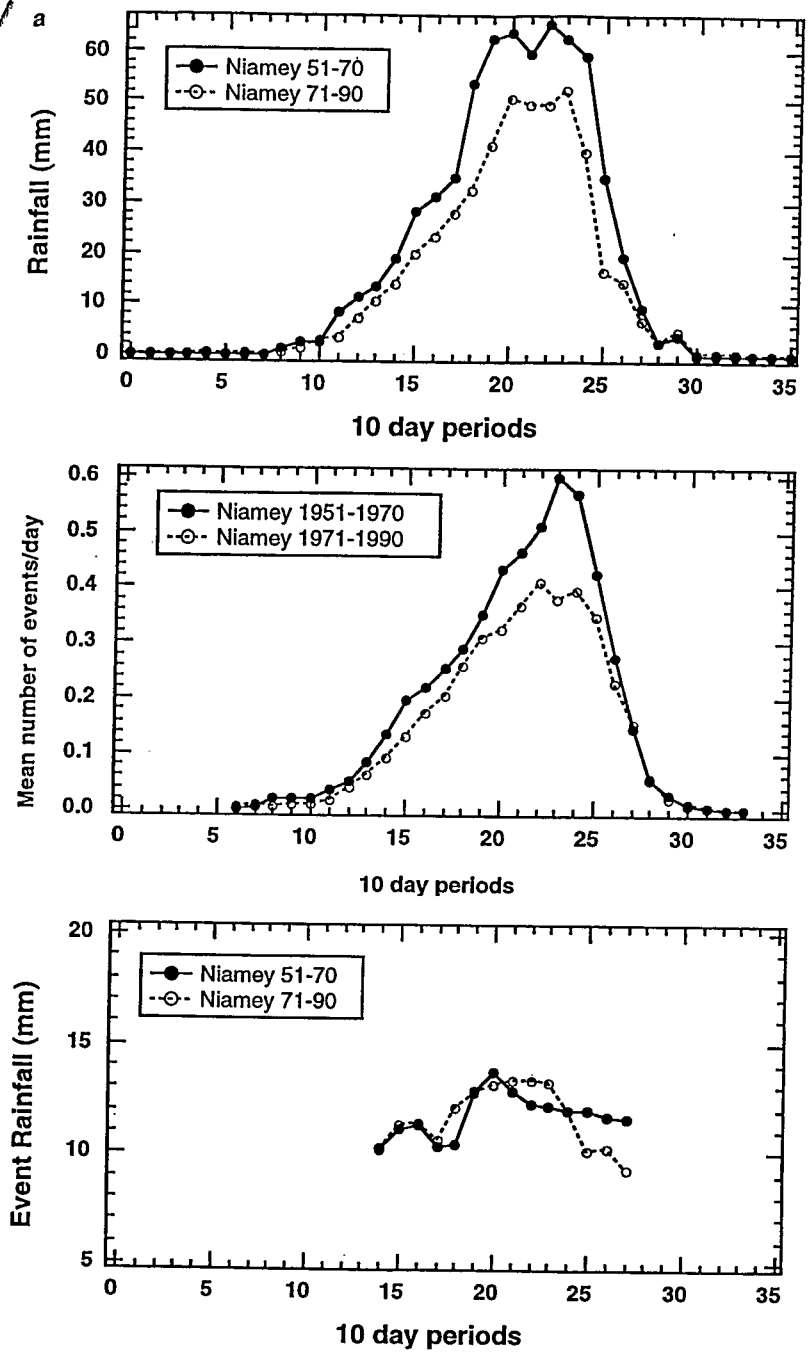

Fig. 3. a Comparison of the seasonal cycles, for the wet period 51–70 and the dry period 71–90 at Niamey (13°30′N, Sahelian climate). Up: the 10-day rainfall; middle: the average number of rain events (n); bottom: the mean event rainfall (h)

and the consequences of the drought in the 70s and 80s were devastating. It is therefore of special interest to check whether the GCM's can reliably reproduce the average Sahelian rainfall climate and its major modes of variability, at least

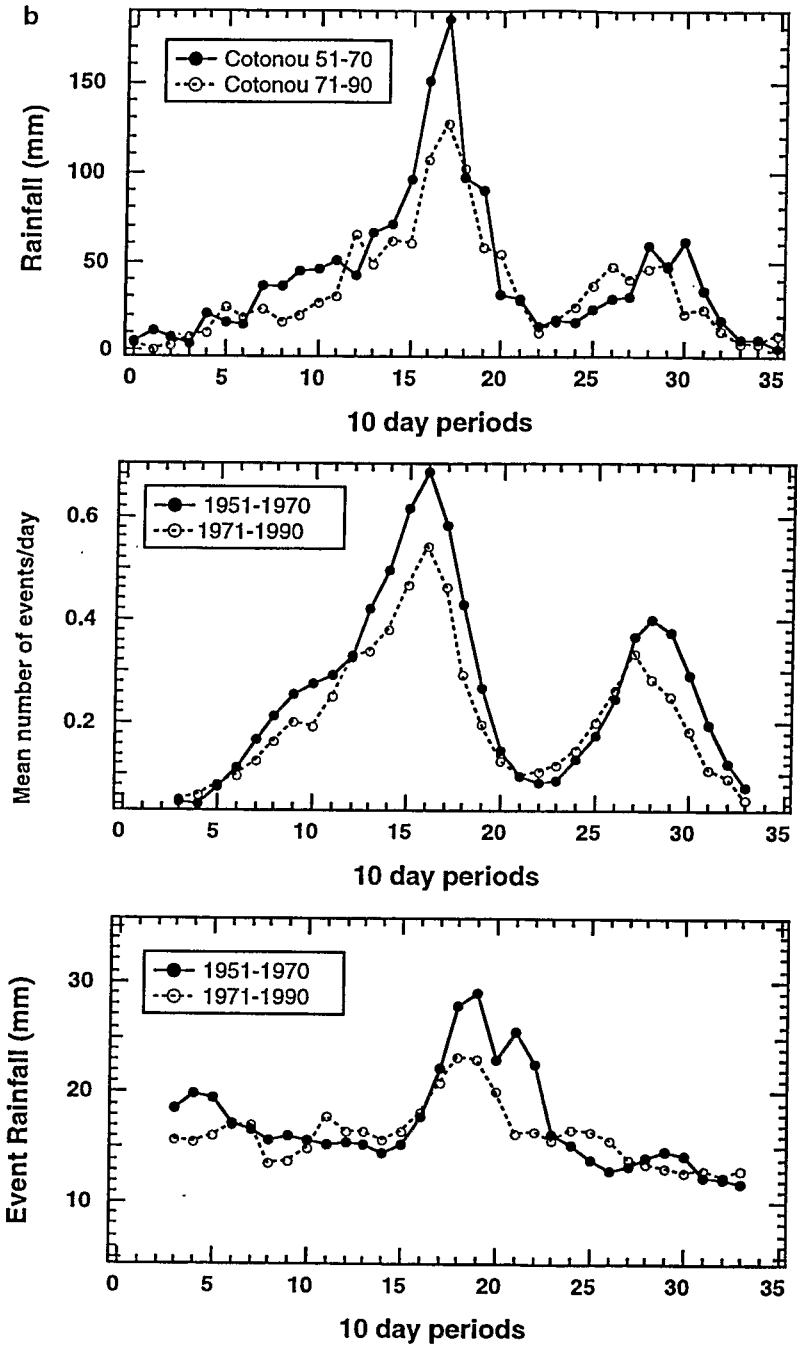

Fig. 3. b Comparison of the seasonal cycles, for the wet period 51–70 and the dry period 71–90 at Cotonou (6°N, coastal climate). Up: the 10-day rainfall; middle: the average number of rain events (n); bottom: the mean event rainfall (h)

those which are supposedly related to large scale atmospheric forcing. The first obvious characteristic of Sahelian rainfall is its continuous and regular decrease when moving from 10°N to its northern desert limit. This gradient is in the order

of 1 to 1.5 mm/km/year. Another basic feature of the Sahelian climate is its single rainy season. Looking at Fig. 3, it seems that the length of this rainy season did not change much during the drought. This may be viewed as an element of stability of the Sahelian climate. Regarding the modes of time variability, two of them are of major importance: the one analysed above which is a decadal mode, and the interannual mode. The ability of a GCM to reproduce these various important characteristics of the Sahelian rainfall regime is reviewed below.

3 Climate modelling

The GCM used here is the version 6 of the LMD-GCM (Polcher and Laval, 1994). This grid-point model is in sine of latitude and has a resolution near the equator of about 1.65° × 3.75°. The vertical structure of the atmosphere is resolved with 15 levels. This version of the model, which is coupled to the land surface scheme SECHIBA (de Rosnay and Polcher, 1998) has been integrated with observed sea surface temperatures over 34 years starting in 1960. The sea surface temperature was taken from the GISST (Global sea-Ice and Sea Surface Temperature) database constructed by the Hadley centre (Rayner et al., 1996). In order to separate in the interannual variability of the simulated climate the part forced by the ocean and the one due to the chaotic nature of the atmosphere, three of these integrations were performed. The only differences between these simulations are the initial conditions used to start the model on 1 January 1960. For a separation of the external from the internal variability of the climate a larger number of integrations are needed (Harzallah and Sadourny, 1995) but here the aim of the ensemble is to give an estimate of the significance of the models' deviation from observations. In the present study we will focus on the Sahelian grid bordered by heavy line in Fig. 5. This mesh (hereafter referred to as the Niamey grid mesh) contains the EPSAT-Niger experimental zone, over which high resolution rainfall observations carried out from 1990 onward are available. The Niamey grid box is delimited by the latitudes 12.83 and 13.47 and by the longitudes 0 and 3.75, thus covering an area of approximately 70,000 km^2.

From the 300 gauges covering the 14° × 12° regional area, a subset of 28 raingauges located on or close to the Niamey grid mesh was extracted. A daily series of area averaged rainfall was computed by kriging the 28 daily point data. The study of Lebel and Amani (1999) shows that with such a density of 28 gauges over 70,000 km^2 the raindepth is estimated with a reasonable accuracy for time steps larger than 10 days. This series may thus be considered as a ground truth to which the GCM outputs are to be compared. Due to difficulties in retrieving the daily observations over Burkina-Faso for the period 1991–1994, we had to limit the comparison to the period 1960–1990. It should be noted at this point that there is a significant internal model variability, as illustrated in Fig. 12 further in the paper. Therefore, we will characterise the general GCM behaviour by averaging the three run outputs, even though, as shown by Venzke et al. (1999), it would require at least a twice larger number of simulations to get a proper estimation of the forced variability. It is not possible to correctly address this point in this paper, but Sect. 5 will illustrate the large differences existing between the three runs.

Latitudinal gradient

The climatologic latitudinal gradient computed from the observations over the period 1951–1990 is in the order of 150 mm per degree of latitude between 12°N and 14°N, and in the order of 120 mm per degree North to 14°N (Fig. 6). The

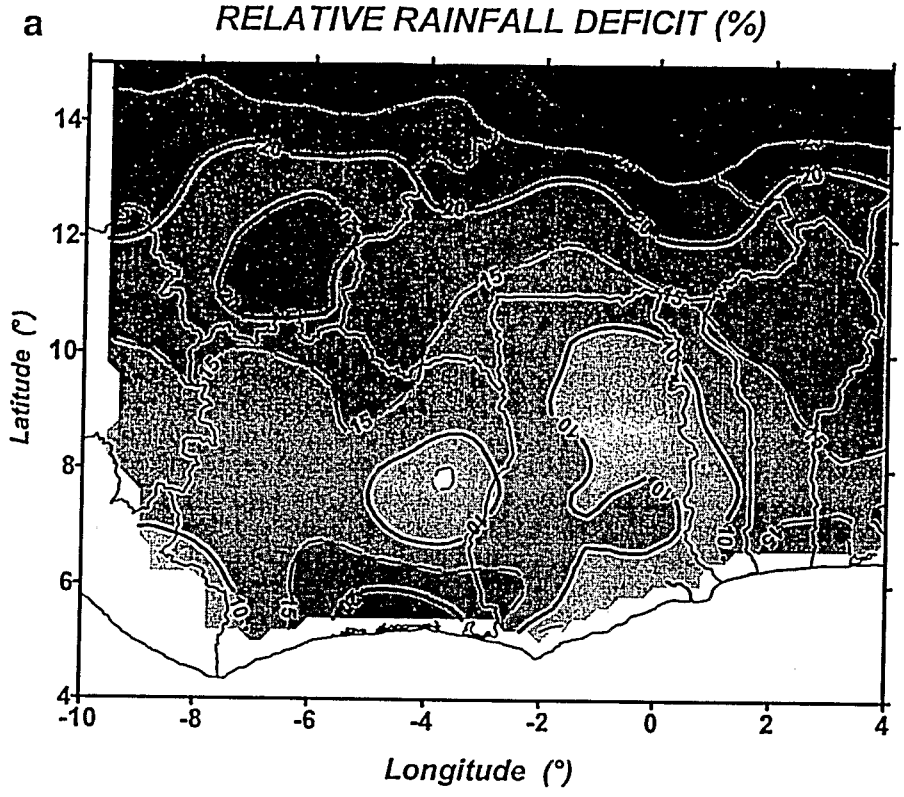
a
RELATIVE RAINFALL DEFICIT (%)
Latitude (°)
Longitude (°)
14
12
10
8
6
4
-10
-8
-6
-4
-2
0
2
4

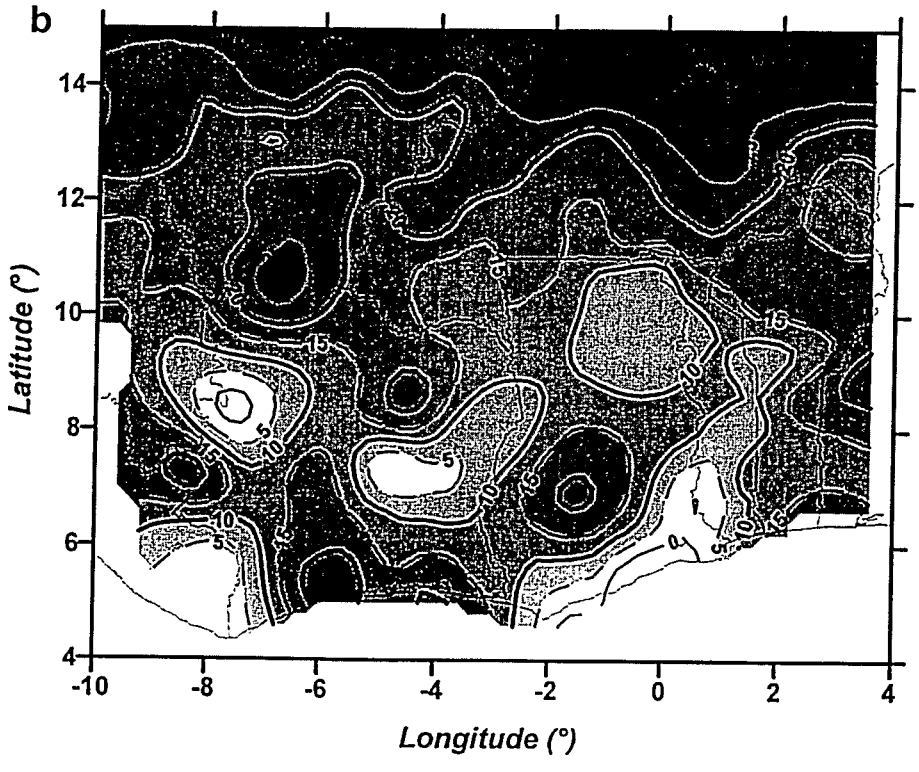
b
Latitude (°)
Longitude (°)
14
12
10
8
6
4
-10
-8
-6
-4
-2
0
2
4

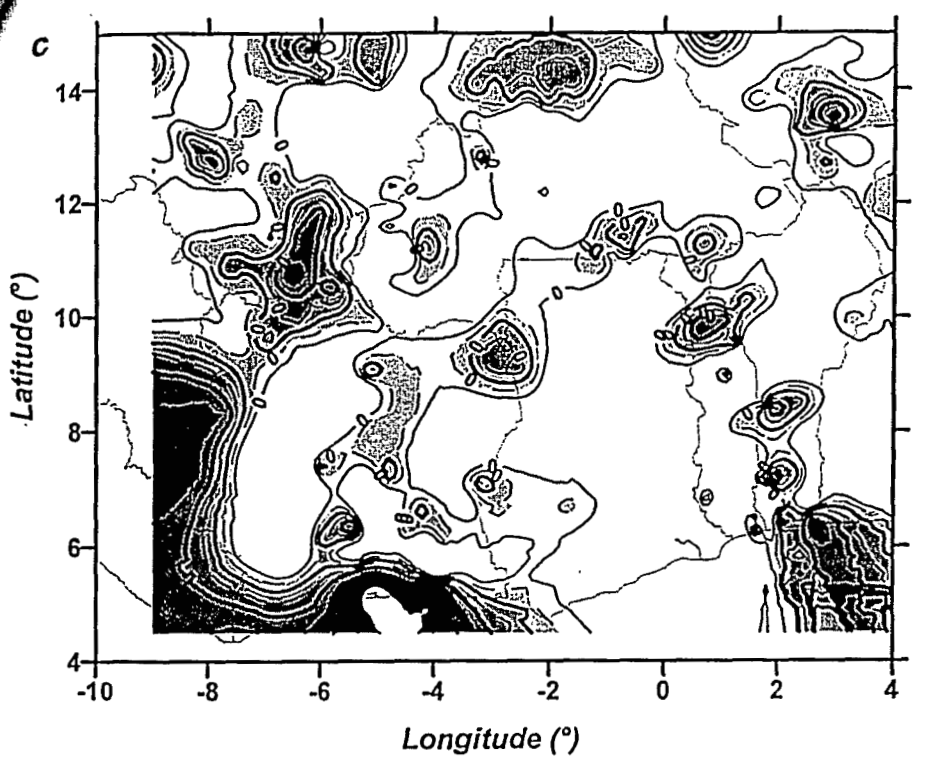

Fig. 4. Regional map of the relative changes of various rain parameters between the wet period P_1 and the dry period P_2: a mean annual rainfall; b mean annual number of events; c mean event rainfall (yearly average). Positive values indicate deficit of P_2 with respect to P_1

GCM produces a rainfall gradient very close to the one observed, albeit a positive offset close to 200 mm. The slight break in the gradient occurring around 13.5°N in the observations is also present in the GCM output. However, when moving North to 14°N, the decrease in the GCM rainfall is smaller than in the observations, resulting in the offset being larger than 250 mm at 15.5°N. In this figure the importance of the internal variability can already be noted. Although the values plotted in the figure are 30-year averages, the three simulations can still be separated. This shows for this region the important role played by the internal variability of the atmosphere.

Seasonal cycle

The observed and GCM-average seasonal cycles are compared in Fig. 7. The two curves were obtained by averaging the 10-day rainfall over the 31 years of the period of study. The model starts the rainy season too early and the increase in precipitation is not rapid enough. It is impossible to determine if this error is caused by a bad representation in the model of the land-surface/atmosphere interactions or if an entire process, which is important for the onset and evolution of the rainy season, is missing. An interesting fact, which has recently been noted, is that this same deficiency is found in other models (Peter Cox, personal communication). This does not mean that GCM's are lacking an essential process but it could be due to the way these models are validated. As the aim of GCM's is to simulate the large scale circulation the diagnostics most often looked at are the

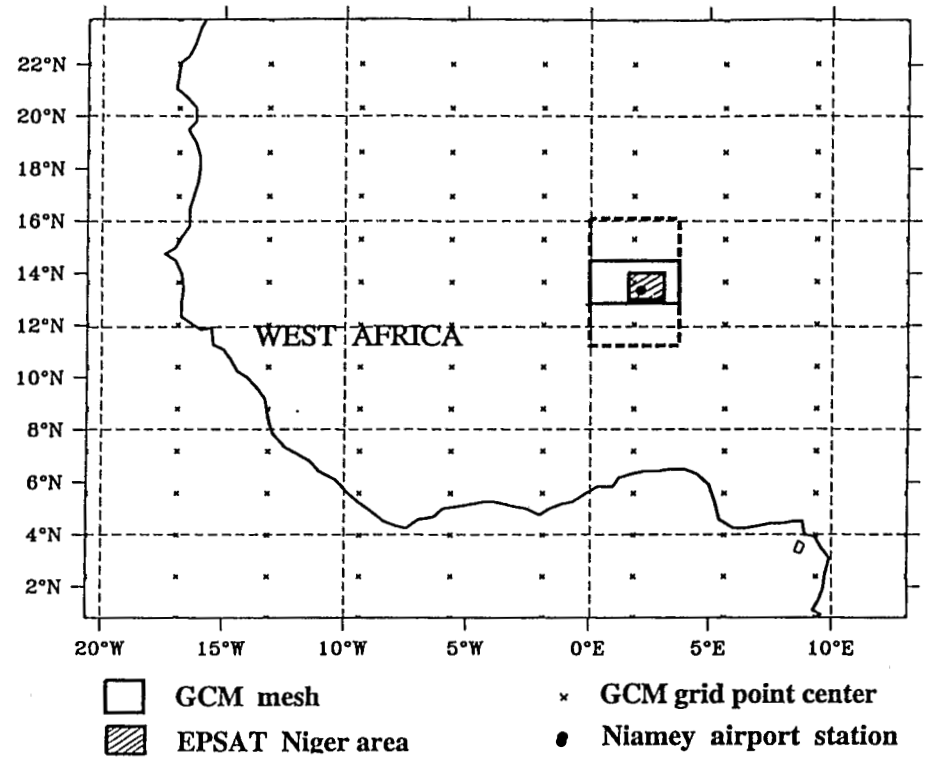

Fig. 5. Location of the Niamey grid mesh (70,000 km^2) of the LMD-6 GCM. The EPSAT-Niger study area (16,000 km^2) is the hatched area located inside the grid mesh

monthly or seasonal mean maps of atmospheric quantities. There is probably a lack of attention paid to the seasonal evolution of regional processes.

Wet years versus dry years

Since there is a large overestimation of the average annual rainfall over the Niamey grid mesh by the GCM, it was decided to scale the observed and the GCM annual series by their respective standard deviation in order to carry out a meaningful comparison of their interannual variability. The two resulting stan-

Table 1. Differences between the observed and GCM rainfalls for the three periods identified in Fig. 7

	Period 1 (decades 1–10)	Period 2 (decades 11–31)	Period 3 (decades 31–36)	Annual
Observed (mm)	4.4	494	0	498
Average GCM (mm)	48.8	662	9.7	720
Total bias (%)	20	75.5	4.5	100

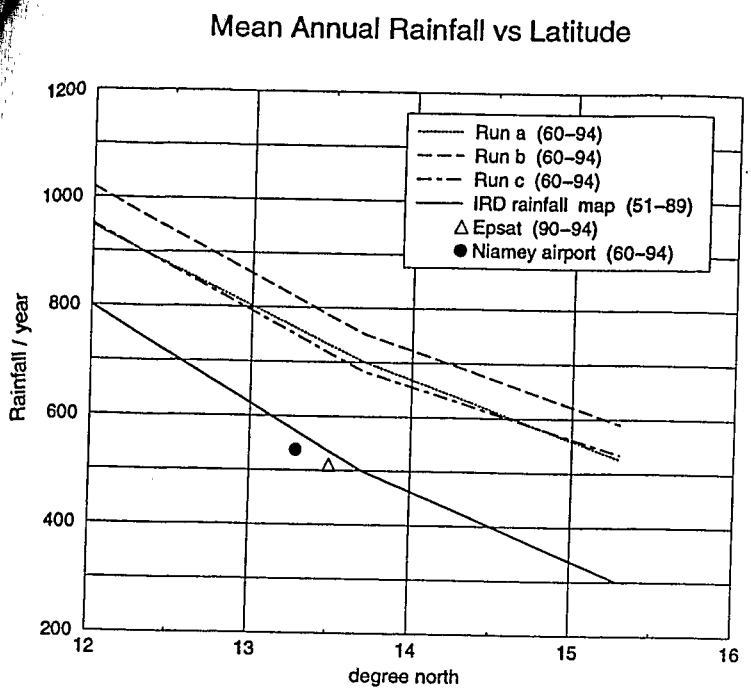

Fig. 6. Comparison of the observed latitudinal rainfall gradient over the Sahel (IRD rainfall map) and the gradient simulated by the three runs of the LMD-GCM. The gradients were computed from zonal averages covering 11.25° in longitude (between 3.75°W and 7.5°E)

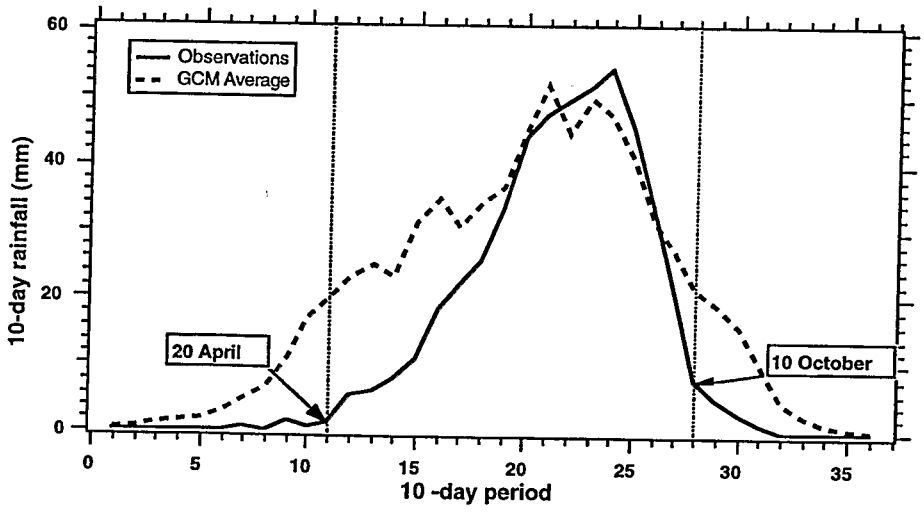

Fig. 7. The seasonal cycle as observed and simulated by the GCM over the Niamey grid mesh. The observed raindepth is obtained by kriging the 28 observations available over or close to the grid mesh

dardised series are represented in Fig. 8. In this figure the observed index series present a pattern slightly different from the one shown by the series of Fig. 1, computed over the whole Sahel for the period 1921–1994. This illustrates how

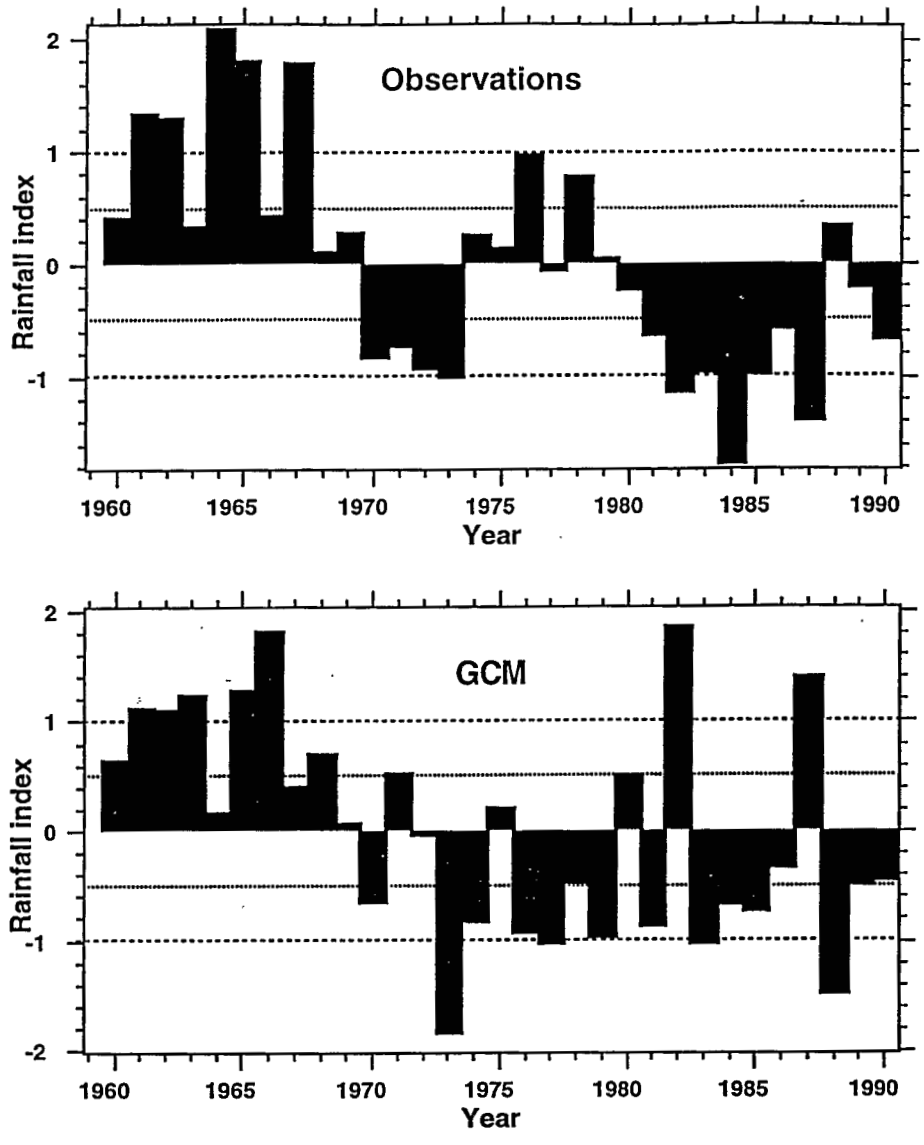

Fig. 8. Interannual variability of rainfall over the Niamey grid mesh, as observed from the network of 28 gauges (top) and as simulated by the average of the three LMD-GCM runs (bottom). The rainfall index is the annual rainfall divided by the average of the series

different samplings in space and time may lead to different visions of the decadal and interannual variabilities in this region. Since the standardisation factor is computed over 31 years (1960–1990) in Fig. 8, whereas it was computed over 74 years in Fig. 1, the years 1974–1979 appear moderately wet in Fig. 8, whereas they are moderately dry in Fig. 1. Nonetheless, the wet years 1960–1969, and the two dry periods 1970–1973 and 1980–1990 are similar in both figures.

When comparing the observed and the GCM index series, two striking points arise: (i) the period 1960–1969 of continuously positive observed index is well reproduced by the GCM; (ii) on the opposite, the ensuing succession of three well identifiable periods (1970–1973, dry; 1974–1979, moderately wet; 1980–1990, dry)

in the observed series is not reproduced by the GCM series. Since the only "dated" informations used in the GCM are the measured SST's, the ability of the GCM to "see" the continuous period of wet years in the 60's, is consistent with the finding of Fontaine et al. (1998) that the slow reversal of the dipolar structure of the near-global ocean – first studied by Folland et al. (1986) -has strengthened since the beginning of the 70's. On the other hand, the important discrepancies detected on given years of the 1970–1990 period between the observed index and the GCM index might be attributed to a dominance of the internal GCM variability or, in other words, to a weak forcing by the SST's. Most notable in that respect are the years 1971, 1982, 1987 and 1988. The first three of these years are markedly dry in the observations whereas they are moderately to extremely wets in the GCM. Year 1982 is the one with the greatest difference: it is the wettest year for the GCM, whereas it was one of the three driest observed years. This discrepancy is not a local matter, since 1982 was severely dry over the whole Sahel as may be seen in Fig. 1. Year 1988 presents another singular behaviour of the GCM. Whereas this year is the only one presenting a positive observed index for the period 1980–1990, it is the second driest year for the GCM over the whole 1960–1990 period. It is worth noting that the years 1971, 1982, 1987 and 1988 are all years with intense ENSO (warm and cold) events. The poor behaviour of the LMD-GCM for these years is in line with the results of previous studies (see e.g., Moron et al., 1998) showing that GCM's have difficulties in reproducing the West African rainfields for extreme ENSO years. While the correlation between the ENSO and the Sahelian rainfall is weak in the observations, it is likely stronger in the GCM's. Ceron and Gueremy (1999) also noted the specific patterns of the atmosphere dynamics over West Africa in 1987. To summarise, there appears to be a dominant interannual variability of the GCM during the period 1970–1990, whereas observations are more dominated by a multi-year persistence. How this mismatch may be attributed to the respective roles of the SST's (weak forcing or wrong representation of the SST patterns) and of the continental surface processes (wrong representation or lack of proper information regarding the surface conditions that play an important role in the triggering of the convection) is a matter of debate and an important topic for future investigation.

4
Observed rainfall variability at hydrological scales

Given the great intermittency of rainfall and runoff in the Sahel, the observations performed in routine by the national services are most often insufficient to address the variability issue at hydrological scales. For instance the network of daily reading raingauges used in Sect. 2 above has an average density of less than 2 gauges for each $1° \times 1°$ square (just less than 6000 km^2 per gauge), whereas the small Sahelian hydrological units have a typical size in the order of 10 to 100 km^2 (see Desconnets et al., 1997). Thanks to the high resolution network setup within the framework of the EPSAT-Niger experiment, it has however been possible to obtain an in-depth idea of the rainfall variability at small scales in this region. The EPSAT-Niger study area, whose location is indicated in Fig. 5, covers 16,000 km^2. A network of a hundred recording raingauges was operated over the area between 1990 and 1993 included. This network was later reduced to 30 gauges that have continuously operated onward. Detailed studies on the space-time variability of the rainfields observed by this experimental network may be found in Lebel and Le Barbé (1997) and in Lebel and Amani (1999). Ten years of data are now available and their analysis largely confirms the results presented in these two papers, as is illustrated in Figs. 9–11 presented below.

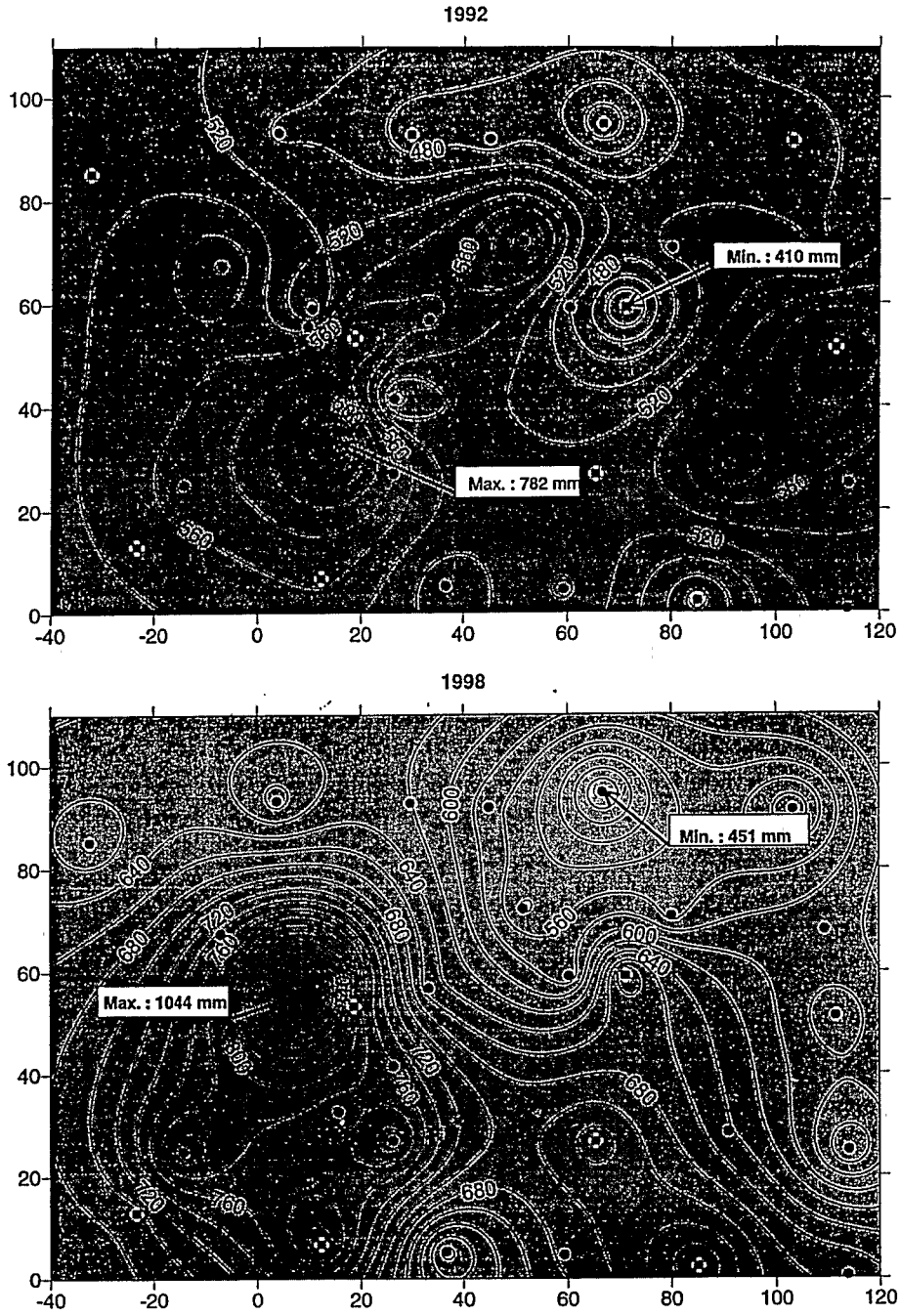

Fig. 9. Seasonal rainfall maps over the EPSAT-Niger study area (1992 and 1998)

In Fig. 9 the seasonal rainfall maps are drawn for 1992 and 1998, where heavy gradients of rainfall were observed: close to 300 mm over 10 km in 1992 and more than 600 mm over 70 km in 1998. Such gradients have a profound impact on the crop yields and surface water available to cattle (in this region most of the

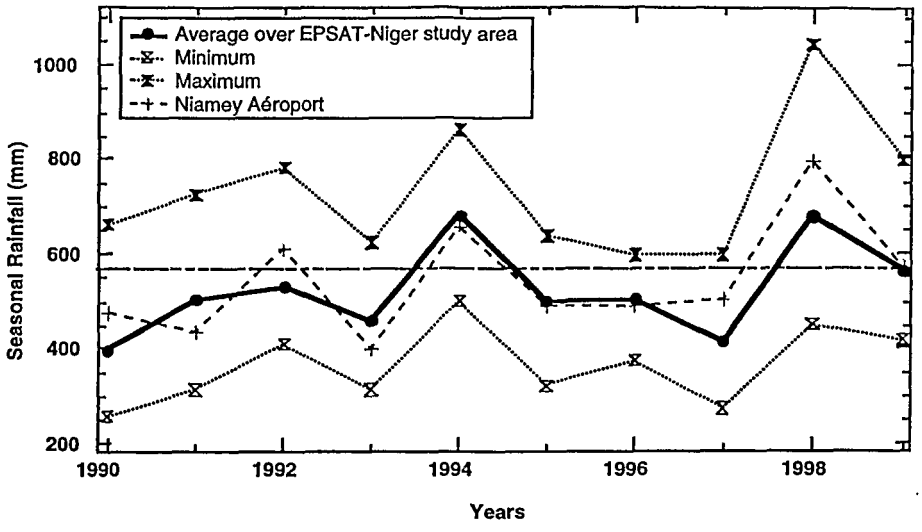

Fig. 10. Interannual variability of the seasonal rainfall over the EPSAT-Niger study area. The dashed line indicates the Niamey average for the period 1950–1989

drinking water is taken from aquifers). Obviously it cannot be expected from any current GCM to catch such gradients, which are nevertheless of crucial importance to understand, model and predict the water resources at the seasonal scale. A synthetic view of the extreme rainfall space variability at the seasonal scale is given in Fig. 10. This figure compares the interannual fluctuations of various seasonal rain indicators: the area average over the whole EPSAT-Niger study area, the minimum point rainfall and the maximum point rainfall recorded on the network and the annual rainfall at the Niamey-Aéroport station. Every year the ratio of the maximum over the minimum is close to two. The comparison of the area average with the values recorded at the Niamey station, commonly used to characterise the rainy season in this region provides additional evidence on the spatial variability at the seasonal scale. The average absolute difference between the two series is 10%, half of the errors being larger than 15% and two of them larger than 20%. This illustrates a previous finding of Lebel and Amani (1999) that, when using a single station to estimate the areal value over the EPSAT-Niger study area, the probability of the estimation error being larger than 20% is around 20%.

Figure 10 also gives some information about the interannual variability. With respect to the 1950–1989 average for Niamey (560 mm), 7 seasons are in deficit and 2 seasons (1994 and 1998) are in excess, when considering the area average. The years 1990–1993 were as dry as the average of the 70s, somewhat wetter than the first halve of the 80s, but dryer than the second halve of the 80s. It seems that the end of the century, starting in 1994, corresponds to a return towards milder conditions.

The high resolution of the EPSAT-Niger data provided some interesting and new clues on the spatial variability of the Sahelian rainfields at the seasonal scale. It also allows a direct and reliable identification of the rain events, thus making possible to characterise the rainfall variability at a relevant hydrological scale, without having to resort to a stochastic model as the one used in Sect. 2. This is illustrated in Fig. 11, displaying the co-fluctuation, over the EPSAT-Niger study area, of the three variables studied in Sect. 2: the annual rainfall (R_Y), the number

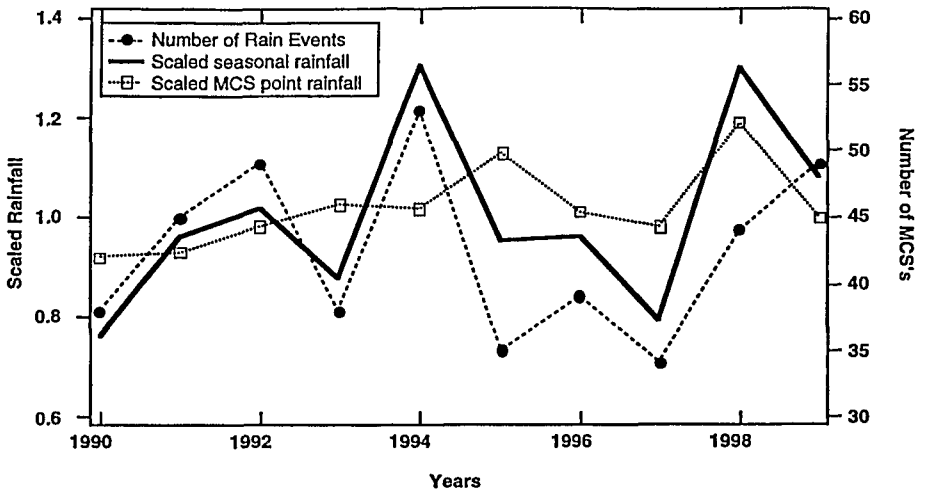

Fig. 11. Interannual variability of the seasonal rainfall, the mean number of events (n) and the mean event rainfall (h) during the EPSAT-Niger years

of events recorded in a year (n_Y) and the mean event rainfall (h_Y) computed over these n_Y events. There is a visible positive correlation between R_Y and n_Y. This correlation is much weaker between R_Y and h_Y. Globally there is thus an indication that the interannual variability of the seasonal rainfall has a larger link with that of the number of events than with that of the mean event rainfall. However this conclusion is not as solidly based as the one obtained in Sect. 2 at the decadal scale. One problem here is the small size of our sample. For instance for the period 1990–1998, the coefficient of determination r^2 between R_Y and n_Y is equal to 0.55, while it increases to 0.63 if the year 1998 is removed. On the opposite, the coefficient of determination r^2 between R_Y and h_Y is equal to 0.29, while it decreases to 0.05 if the year 1998 is removed.

Quantifying the links between the fluctuations of R_Y, n_Y and h_Y has implications going further than the above statistical considerations. As a matter of fact, a study carried out by Laurent et al. (1997) showed that the list of rain events identified from the EPSAT-Niger data set are in good agreement with the list of mesoscale convective systems (MCS) seen by the infrared channel of Meteosat. The EPSAT-Niger events may thus be viewed as a measure of the average intensity and frequency of organised deep convection in the Niamey area. Rainfall variability over this area being predominantly linked to the occurrence rate of deep organised convection – while the average intensity of the associated rainfields varies little by comparison – is a fact that we should be able to track in atmospheric models. The exact meaning of this result is not absolutely clear at the moment. However, since there is a strong and commending signal at the decadal scale with its counterpart, even though weaker, at the interannual scale, it has to be looked at in the simulations by the LMD-GCM.

5
The mesoscale convective systems in the GCM

In order to illustrate in which way the GCM is producing biased rainfall outputs, leading to the erroneous overall statistics discussed in Sect. 3, the observed daily rainfall signal and the 3 daily signals corresponding to each run of the GCM are shown in Fig. 12 for the year 1982. Remember from Sect. 3 that this year is the

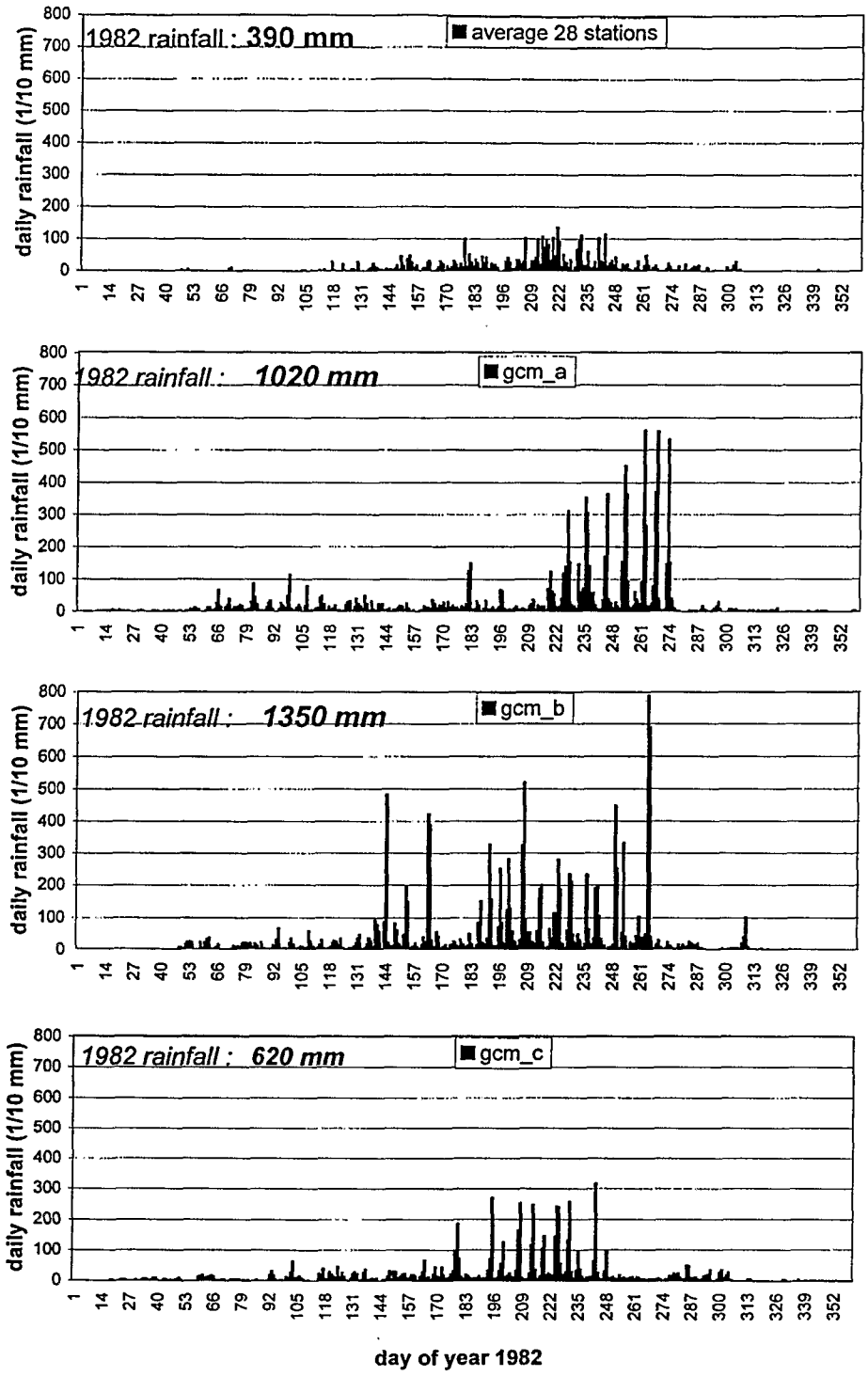

Fig. 12. Daily rainfall of 1982, as observed by the network of 28 raingauges and as simulated by each of the 3 runs of the LMD-GCM

one displaying the largest difference between the standard rainfall index of the observed 31-year series and the standard rainfall index of the average GCM series. It is therefore not surprising to see that the average GCM rainfall (997 mm) for that year is almost three times as large as the observed rainfall (390 mm). It is also worth noting that there are great differences between the three runs. It appears that the GCM has difficulties to simulate this year, for some undetected reason. Looking to the daily signal we see that: (i) all three runs produce a large number of daily rains greater than 10 mm, whereas there are only a couple of them in the observed signal; (ii) the two wettest runs (run a and run b) produce several daily rainfall larger than 50 mm, whereas the largest daily rainfall in the observed series is 11.7 mm; (iii) there is no correspondence in the timing of the large daily rainfalls from one series to another. The fact that a few unrealistic daily rainfalls explain a great deal of the GCM bias is summarised by the following statistics: the five largest values account for 14% of the seasonal total in the observed series, and between 22 and 24% in the GCM series (a remarkably stable percentage); the ten largest values account for 26% of the seasonal total in the observed series, and between 35 and 41% in the GCM series; the same ten largest values account for 40–50% of the total difference between the annual observed rainfall and the GCM annual rainfall.

The dominant weight of daily rainfalls larger than 20 mm in producing the GCM rainfall bias is not restricted to the sole 1982 year. Looking at statistics over the whole period of study shows that in 31 years of observations there were only 4 days with a grid mesh area average greater than 30 mm and none with a grid mesh area average greater than 40 mm. At the same time, the three GCM simulations produce an average of 74 days with rainfall greater than 30 mm and an average of 36 days with rainfall greater than 40 mm (see Fig. 13). Altogether daily observed rainfalls larger than 20 mm represent a total of 34 mm per year – associated with a total of 43 days, or 1.4 per year, while the daily GCM rainfalls larger than 20 mm represent a total of 211 mm per year – associated with a total of 187 days, or 6 per year. The GCM surplus of 177 mm is very close to the difference of 168 mm that was computed in Table 1 between the GCM rain and the observed rain over the rainy season (defined as the period covering the

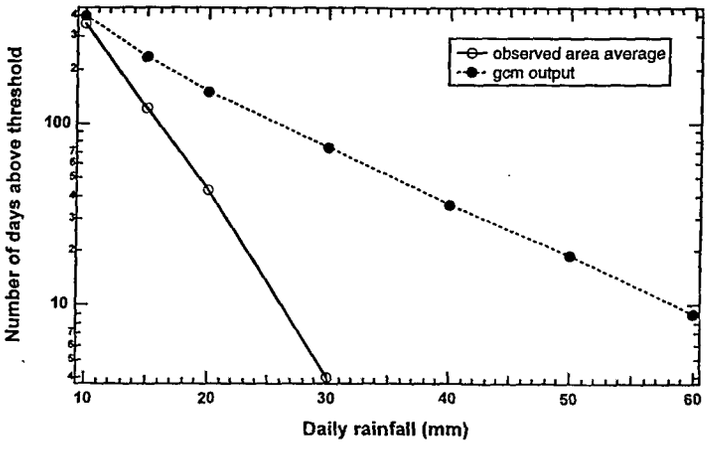

Fig. 13. Distribution function of daily rainfall above 10 mm for the GCM outputs (average over the three runs) and the observations

Table 2. Distribution of observed and GCM daily rainfall. Four classes of daily rainfall are defined. In the last line, the difference (GCM – observations) for each class is computed as a percentage of the average interannual GCM bias (222 mm, see Table 1)

Thresholds (mm)	<1	1–10	10–20	>20
Number of days (observations, 31 years)	8368	2442	311	43
Number of days (GCM, 31 years)	6927	3831	219	187
Observed cumulative rainfall (mm/year)	21.4	308.7	134.1	33.7
GCM cumulative rainfall (mm/year)	55.9	352.1	101.0	211.0
Relative bias of the GCM (%)	15.5	19.5	−14.9	79.9

decades 11–31 included). Since almost all GCM daily rainfall larger than 20 mm are recorded during the rainy season a double conclusion comes up:

(i) the total average GCM rainfall bias (222 mm/year) has two components: one is linked to the precipitations occurring during the dry season, accounting for 25% of the total and associated with rains that very rarely exceeds 10 mm and never exceeds 20 mm/day; the other is precipitations occurring during the rainy season, accounting for 75% of the total, that is 168 mm;

(ii) the rainy season bias of 168 mm is almost entirely caused by the daily rainfalls larger than 20 mm, as may be seen from Table 2; whereas the number of days with rainfall in between 1 and 20 mm differs by less than 10% when comparing the GCM and the observation series, the GCM is producing four times too many rainy days with rainfall over 20 mm.

If one considers that heavy daily rainfalls are associated with convective events, the above numbers show that, in general, when the GCM triggers convection it is too strong. This results questions our ability to model convection on the scales of GCM's. The convection schemes used in the present GCM are rather simple (Kuo, 1965; Manabe and Strickler, 1964) and it has to be seen if more complex parameterisations, which deal with sub-grid variability of convection, do produce at these scales the right frequency and intensity of events. A condition for a correct simulation of the spectrum of convective events in the tropics over continents is that sufficient information is available at the large scale to parameterise correctly the triggering and evolution of the systems. This has still to be determined and the present data set when used to validate other GCM's will certainly help answer these questions.

6
Conclusion

Being the only tools presently available for the simulation of possible climatic scenarios of the future, GCM's constitute the basis for studying the hydrological impact of climate variability. However the relevance of such impact studies are conditioned to a preliminary verification that the rainfall produced by GCM's is not affected by bias that will propagate in the hydrological cycle. This paper summarises a preliminary investigation of the quality of the LMD-GCM rain outputs for a Sahelian grid mesh covering 1.65° × 3.75°, over the period 1960–1990. It was found that these outputs are indeed affected by a number of bias, that are not limited to an unrealistic representation of the rainfall distribution in space.

First, the rainy season is too long. During the first 100 days of the year, the observed rainfall climatology is 4 mm, while the GCM produces 49 mm. During the last 60 days, the respective numbers are 0 mm for the observations and 10 mm for the GCM. During the 200 days of the rainy season, the GCM produces 662 mm against an observed average of 494 mm. Thus, the GCM overestimates the total annual rainfall by 222 mm, 25% of this number being during the dry season and 75%, (168 mm), during the rainy season. Looking at daily rainfall statistics it is seen that there are four times as many rainy days with a rainfall over 20 mm in the GCM as there are in the observations. This means a GCM positive bias of 176 mm per year. This bias is concentrated during the rainy season and its value is very close to the total rainy season bias (168 mm). It thus appears that, even though the distributions of GCM and Observed daily rainfalls are not exactly similar for daily rains under 20 mm, it is the large discrepancy for daily rains over 20 mm which is almost totally responsible of the overall rainy season GCM bias. In conclusion, as far as the seasonal cycle is concerned, there are two major sources of errors in the GCM: (i) it produces significant rainfall during the dry season; (ii) during the rainy season it generates much too intense convective systems.

Of the two above errors, one, the dry season rain, is of limited concern for hydrological predictability, whereas the second, the much too intense convective systems poses a major problem. Rainfall during the dry season is probably associated with some local recycling of an excess of humidity remaining present at the end of the rainy season. This rain is easy to discard in hydrological studies. On the other hand, the common assumption that, in a hydrologic perspective, the main limitation of GCM outputs were related to their space averaging seems to be non longer valid. For instance, Lebel et al. (1998) have developed a stochastic disaggregation model able to produce, from a large spatial average, rainfields at relevant space-time scales for hydrological studies. The idea underlying this approach was that GCM's could produce realistic convective systems, whether considering their intensity and rate of occurrence. The study reported here shows that the large scale rainfalls produced by the Sahelian convective systems in the GCM's have first to be improved before they can be used as inputs to a disaggregation model.

Interesting and question-raising conclusions may also be drawn from the analysis of the interannual and decadal variabilities of the GCM rainfall. During the first third of the simulation period (1960–1969), which is the end of a 2-decade wet phase, the GCM behaves very well. Then, when entering a globally dry phase for two decades (1970–1990), the interannual variability is seriously disturbed in the GCM as compared to what it is in the observations. A few years are very badly simulated (especially 1982 and 1987). Several reasons, not exclusive one from each other, may explain this: (i) large internal variability of the atmosphere making the study of 3 runs over a single grid mesh not sufficient to reach the average behaviour of the GCM; (ii) weak forcing by the SST's; (iii) oversimplified representation of the land-surface processes in the GCM, especially those linked to the triggering and development of the convection.

Obviously this validation of GCM rainfall outputs over a range of scales is far from complete. The aim of this paper was to draw attention to the necessity of performing such studies. Our goal is now to reach more precise conclusions by working in three directions: (i) use of two additional runs in order to better appreciate the influence of the internal variability of the GCM itself; (ii) enlargement to a wider Sahelian domain and to areas governed by Sudanian and Guinean climates.

References

Ceron JP, Gueremy JF (1999) Validation of the space-time variability of African Easterly Waves simulated by the CNRM GCM. J. Climate, 12: 2831–2855

Desconnets JC, Taupin JD, Lebel T, Leduc C (1997) Hydrology of the HAPEX-Sahel central Super-Site: surface water drainage and aquifer recharge through the pool systems. J. Hydrol., 188–189, 155–178

Folland CK, Palmer TN, Parker DE (1986) Sahel rainfall and worldwide sea temperature 1901–1985. Nature, 320: 602–607

Fontaine B, Janicot S (1996) Sea surface temperature fields associated with West African rainfall anomay types. J. Climate, 9: 2935–2940

Fontaine B, Trzaska S, Janicot S (1998) Evolution of the relationship between near global and Atlantic SST modes and the rainy season in West Africa: statistical analyses and sensitivity experiments. Climate Dynamics, 14: 353–368

Harzallah A, Sadourny R (1995) Internal versus SST-forced variability as simulated by an atmospheric general circulation model. J. Climate, 8: 474–495

Hastenrath S (1990) Decadal-scale changes of the circulation in the tropical Atlantic sector associated with Sahel drought. Int. J. Climatol., 10: 881–892

Janicot S (1992) Spatio-temporal variability of West African rainfall; Part I: Regionalisations and typings. J. Climate, 5: 489–497

Janowiak JE (1988) An investigation of interannual rainfall variability in Africa. J. Climate, 1: 240–255

Kuo HL (1965) On formation and intensification of tropical cyclones through latent heat release by cumulus convection. J. Atmos. Sci., 22: 40–63

Kushnir Y (1994) Interdecadal variations in North Atlantic SST and associated atmospheric conditions. J. Climate, 7: 141–157

Laurent H, Lebel T, Polcher J (1997) Rainfall variability in Sudano-Sahelian Africa studied from raingauges, satellite and GCM. Proc. 13th conference on hydrology of the 77th AMS Annual meeting, 2–7 February 1997, pp. 17–20. AMS Publ., Long Beach, USA

Le Barbé L, Lebel T (1997) Rainfall climatology of the HAPEX-Sahel region during the years 1950–1990. J. Hydrol., 188–189: 43–73

Lebel T, Le Barbé L (1997) Rainfall monitoring during HAPEX-Sahel: 2. Point and areal estimation at the event and seasonal scales. J. Hydrol., 188–189, 1–4, 97–122

Lebel T, Braud I, Creutin J-D (1998) A space-time disaggregation model adapted to Sahelian squall lines. Water Resources Research, 34(7): 1711–1726

Lebel T, Amani A (1999) Rainfall estimation in the Sahel: what is the ground truth? J. Appl. Meteor., 38: 555–568

Manabe S, Strickler RF (1964) Thermal equilibrium of the atmosphere with a convective adjustment. J. Atmos. Sci., 21: 361–385

Moron V, Navarra A, Ward MN, Roeckner E (1998) Skill and reproducibility of seasonal rainfall patterns in the tropics in ECHAM-4 GCM simulations with prescribed SST. Climate Dynamics, 14: 83–100

Polcher J, Laval K (1994) A statistical study of regional impact of deforestation on climate of the LMD-GCM. Climate Dynamics, 10: 205–219

Rayner NA, Horton EB, Parker DE, Folland CK, Hackett RB (1996) Version 2.2 of the Global sea-Ice and Sea Surface Temperature Data Set, 1903–1994. Climate Research Technical Note 74, unpublished document available from Hadley Centre

de Rosnay P, Polcher J (1998) Improvements of the representation of the hydrological exchanges between the biosphere and the atmosphere in a GCM. Hydrol. Earth Syst. Sci., 2: 239–256

Venzke S, Allen MR, Sutton RT, Rowell DP (1999) Atmospheric response over the North Atlantic to decadal changes in sea surface temperature. J. Climate, 12: 2562–2584